Figure 5. Dapagliflozin inhibits oxidative stress in the kidney. (A, B) ROS production was detected by fluorescence microscopy using dihydroethidium (DHE) staining. ROS was predominantly localized in the interstitia of *db/db* mice, and was suppressed in the *db/db*+dapa groups compared with that in the *db/db* group. Original magnification, ×100. Data are mean ± SEM. *$P<0.05$. (C, D) Localization of Nox4 was detected by immunohistochemistry. The expression of Nox4 was predominantly localized in the interstitia of *db/db* mice, and was suppressed in the *db/db*+dapa groups compared with that in in the *db/db* group. Original magnification, ×100. Data are mean ± SEM. *$P<0.05$.
doi:10.1371/journal.pone.0100777.g005

Inflammatory Gene Expression in the Renal Cortex

qRT-PCR analysis of kidney tissue revealed that the expression of several proinflammatory genes, including *TGF-β*, *MCP-1*, *osteopontin* and *ICAM-1*, was significantly increased in the *db/db* group, but suppressed by dapagliflozin in the *db/db*+1.0 dapa group (Fig. 4A–D).

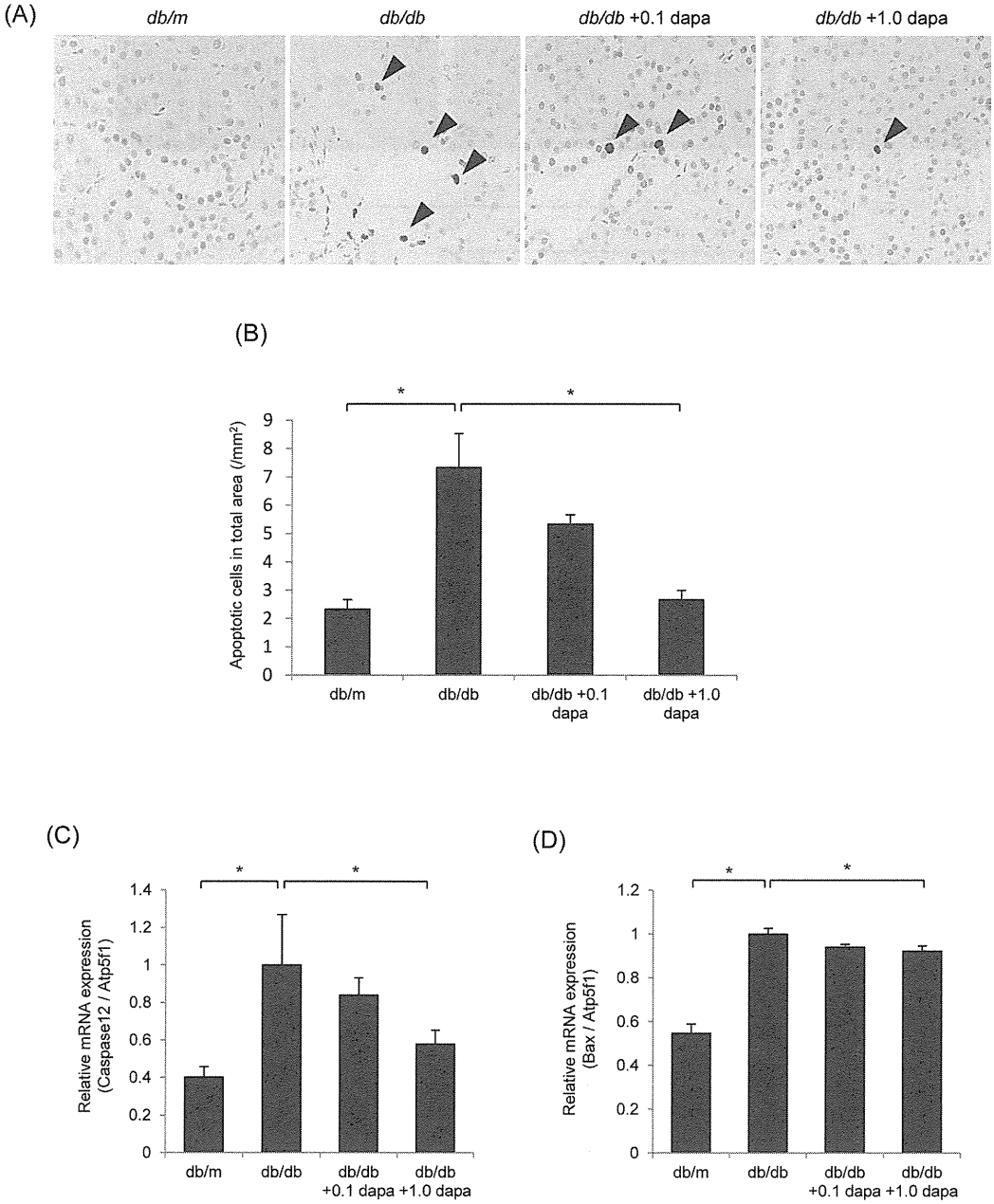

Figure 6. Dapagliflozin inhibits apoptosis in the kidney. (A, B) Apoptosis was detected by TUNEL staining. Arrowheads indicate the apoptotic nuclei. The number of apoptotic cells was higher in the interstitia of *db/db* mice than in *db/m* mice, and was lower in the *db/db*+dapa groups than in the *db/db* group. Original magnification, ×400. Data are mean ± SEM. *$P<0.05$. (C, D) Dapagliflozin reduced the mRNA levels of *Caspase-12* and *Bax* in the kidney. mRNA levels were normalized against *Atp5f1* expression. Data are mean ± SEM. *$P<0.05$.
doi:10.1371/journal.pone.0100777.g006

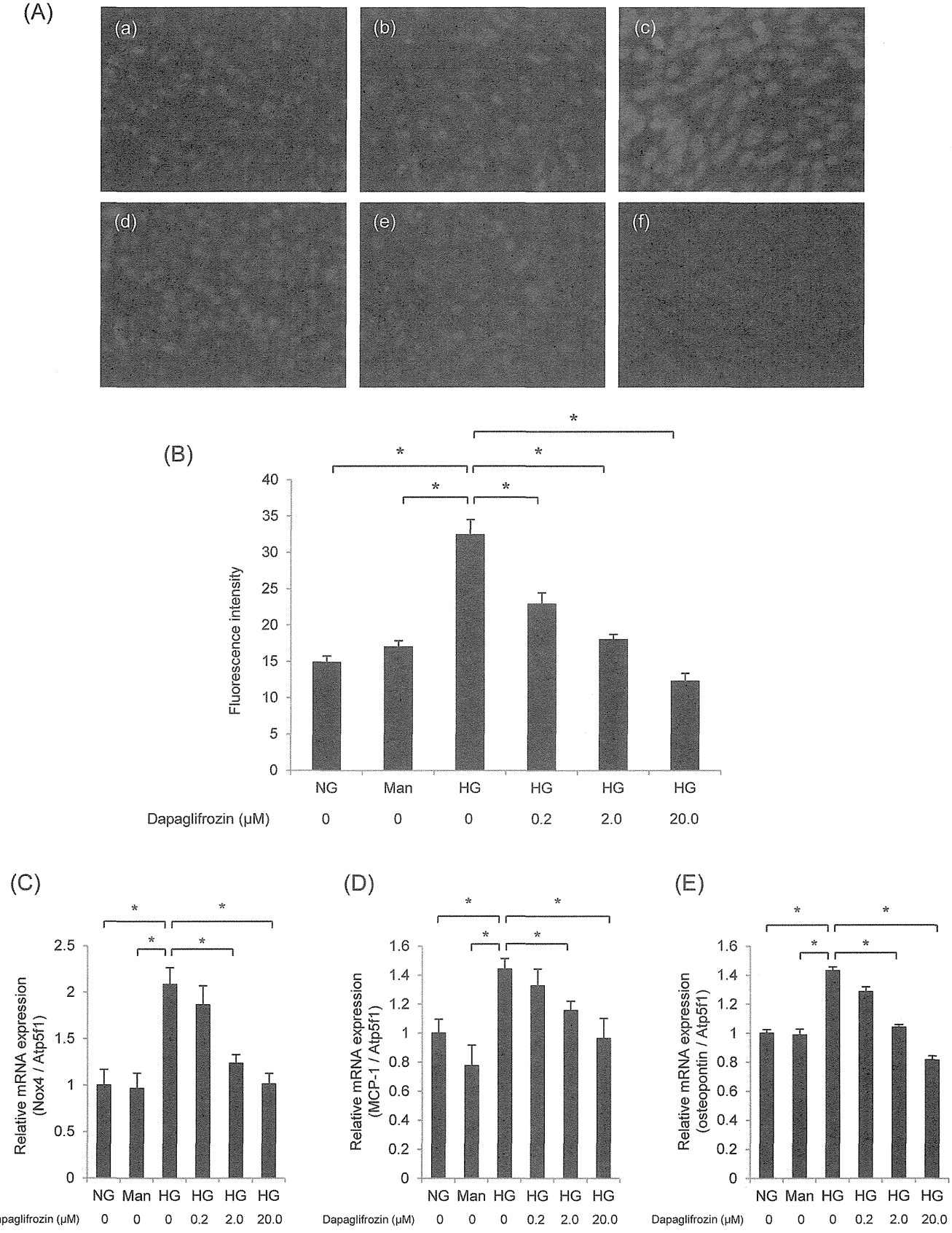

Figure 7. Dapagliflozin suppresses oxidative stress and inflammatory gene expression in cultured proximal tubular epithelial cells. (A) ROS production was detected by fluorescence microscopy using dihydroethidium (DHE) staining. ROS production was not increased by mannitol (b) compared with normal glucose (a), but was increased by high glucose (c). High-glucose-induced ROS production was decreased by dapagliflozin

pretreatment in a dose-dependent manner (d: 0.2 nM; e: 2.0 nM; f: 20.0 nM). (B) Densitometric quantification of ROS production. Data are mean ± SEM. *$P<0.05$ vs. high glucose; NG: normal glucose; Man: mannitol; HG: high glucose; dapa: dapagliflozin. Quantitative RT-PCR analysis of the expression of *Nox4* (C), *MCP-1* (D) and *osteopontin* (E) showed that dapagliflozin inhibited diabetes-induced inflammation in the kidney. mRNA levels were normalized against *Atp5f1* expression. Data are mean ± SEM. *$P<0.05$.
doi:10.1371/journal.pone.0100777.g007

Oxidative Stress and Apoptosis in the Kidney

To investigate the role of oxidative stress and apoptosis, and the effects of dapagliflozin on the pathogenesis of diabetic nephropathy, we conducted DHE staining, Nox4 immunostaining and the TUNEL assay on the kidney. ROS production, which was detected by DHE, was higher in the cortex of the *db/db* group than in that of the *db/m* group, but it was lower in the *db/db*+0.1 and *db/db*+1.0 dapa groups (Fig. 5A and B). Similarly, Nox4, a subunit of NADPH oxidase, was upregulated in the cortex of the *db/db* group, but its expression was attenuated in the *db/db*+1.0 dapa group (Fig. 5C and D). TUNEL staining confirmed that apoptosis was promoted in the *db/db* group, and that dapagliflozin markedly decreased the number of apoptotic cells (Fig. 6A and B). Furthermore, dapagliflozin markedly reduced the high gene expression of the proapoptotic factors, *Caspase-12* and *Bax*, in the *db/db* group (Fig. 6C and D). These data indicate that diabetes increases oxidative stress and apoptosis, and that oxidative stress and apoptosis are suppressed by dapagliflozin.

Oxidative Stress and Inflammatory Gene Expression in Cultured Proximal Tubular Epithelial Cells

To evaluate high-glucose-induced ROS production in cultured proximal tubular epithelial cells, we performed DHE staining. High-glucose medium increased ROS production in mProx24 cells, and dapagliflozin treatment significantly attenuated this increase (Fig. 7A and B). qRT-PCR analysis of mProx24 cells demonstrated that *Nox4* expression induced by high glucose stimulation was also suppressed by dapagliflozin (Fig. 7C). Similarly, the gene expression of *OPN* and *MCP-1* was upregulated by exposure to high glucose and attenuated by dapagliflozin (Fig. 7D and E). These findings suggest that dapagliflozin ameliorates oxidative stress and inflammation induced by high glucose in renal proximal tubular epithelial cells.

Effect of Dapagliflozin on β-cell Mass in *db/db* Mice

We evaluated the effect of dapagliflozin on β-cell morphology by immunoperoxidase staining of insulin (Fig. 8A). The β-cell mass was significantly lower in the *db/db* group compared with that in the *db/m* group at 20 weeks of age. However, dapagliflozin treatment significantly prevented the decrease in β-cell mass in a dose-dependent manner (Fig. 8B).

Discussion

In the present study, we demonstrated that dapagliflozin, a novel SGLT2 inhibitor, suppressed hyperglycemia and restored β-cell mass in diabetic *db/db* mice. Administration of dapagliflozin reduced macrophage infiltration and the gene expression of

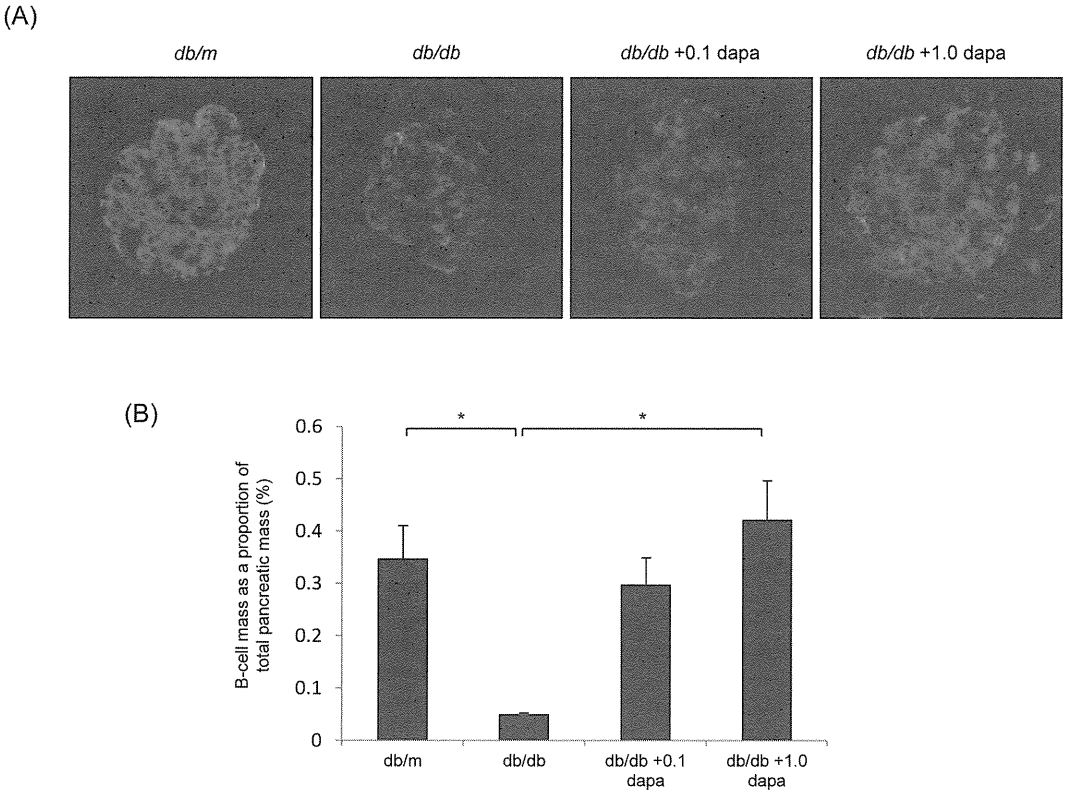

Figure 8. Treatment with dapagliflozin increases β-cell mass in *db/db* mice. (A) Representative immunofluorescent staining of insulin in pancreatic sections derived from *db/m*, *db/db*, and *db/db* with 0.1 or 1.0 mg/kg dapagliflozin mice. Original magnification, ×400. (B) The β-cell area is shown as a proportion of the area of the entire pancreas. Data are mean ± SEM. *$P<0.05$.
doi:10.1371/journal.pone.0100777.g008

inflammation, including *OPN*, *MCP-1* and *TGF-β* in the kidney of diabetic *db/db* mice. Moreover, oxidative stress and apoptosis were lower in the dapagliflozin-treated *db/db* mice than in the untreated mice. Our findings revealed that dapagliflozin exhibits potent antihyperglycemic effects and slows the progression of diabetic nephropathy.

Inhibitors of SGLT2 are newly developed antidiabetic agents and interfere the pathway of physiological glucose reabsorption in the kidney. At present, many preclinical and clinical studies of dapagliflozin, a selective SGLT2 inhibitor, have revealed that selective inhibition of SGLT2 is beneficial for type 2 diabetic patients independently of pancreatic β-cell function or insulin sensitivity, and that the kidney is a safe and effective target for treatment [20]. Although many studies in animals and humans have demonstrated that SGLT2 inhibitors reduce hyperglycemia measurements, including HbA1c, fasting and postprandial glucose, the effects of SGLT2 inhibitors on the organs are not well known. Several studies have demonstrated that genetic and pharmacological inhibition of SGLT2 preserve pancreatic β-cell function [15,21,22]; however, the effects of SGLT2 inhibitors on renal structures and function are not understood. Therefore, we investigated how dapagliflozin influences the progression of diabetic nephropathy using a mouse model of type 2 diabetes.

Inflammation is associated with the development of diabetic nephropathy, and targeting inflammation could be a therapeutic approach for the management of diabetic nephropathy [3,23]. We have demonstrated that activation of nuclear hormone receptors, including peroxisome proliferator-activated receptor (PPAR) γ, PPARδ and liver x receptor, inhibits macrophage infiltration and inflammation, and ameliorates diabetic nephropathy in animal models [16,24,25]. In the present study, dapagliflozin decreased F4/80-positive macrophage infiltration into the kidney in a dose-dependent manner, and suppressed the gene expression of the proinflammatory M1 macrophage marker, *CD11c*, but not the anti-inflammatory M2 macrophage marker, *CD206*. Similarly, dapagliflozin suppressed the gene expression of the chemokine *MCP-1*, the adhesion molecule *ICAM-1*, and the cytokines *OPN* and *TGF-β*. Moreover, our *in vitro* experiments demonstrated that dapagliflozin inhibited the expression of *MCP-1* and *OPN* in mProx24 cells. These results indicate that dapagliflozin inhibits proinflammatory macrophage infiltration and inflammation in diabetic nephropathy.

Numerous studies have also reported an importance for oxidative stress and apoptosis in the pathophysiology of diabetic nephropathy [2,26]. To investigate the effects of dapagliflozin in the etiology of diabetic nephropathy, Oxidative stress in the kidney was evaluated by assessing ROS generation. DHE staining revealed that compared with the non-diabetic *db/m* mice ROS were increased in the interstitia of the diabetic *db/db* mice. The intensity of DHE staining was lower in the dapagliflozin-treated *db/db* mice than in the control *db/db* mice. We also performed immunohistochemistry of Nox4 in diabetic kidney as a promoter of ROS generation. The fact that Nox4 expression was upregulated in diabetic *db/db* mice and decreased by the administration of dapagliflozin suggests that dapagliflozin may reduce oxidative stress by suppressing Nox4-derived ROS generation in the kidney of *db/db* mice. Furthermore, we evaluated apoptosis in the kidney by TUNEL staining and quantitative analysis of gene expression of proapoptotic factors. The number of diabetes-induced apoptotic cells was lower in the dapagliflozin-treated *db/db* mice compared with that in the control *db/db* mice. Similarly, the expression levels of *Caspase-12* and *Bax* were suppressed by the administration of dapagliflozin. Finally, we performed an *in vitro* experiment and revealed that dapagliflozin suppressed the high-glucose-induced ROS generation and *Nox4* expression in cultured mProx24 cells. Taken together, these findings suggest that dapagliflozin suppresses diabetes-induced oxidative stress and apoptosis in the kidney of *db/db* mice.

To date, no studies have evaluated the effect of SGLT2 inhibitors on the progression of diabetic nephropathy in detail, and only two studies have reported renoprotective effects of SGLT2 inhibitors. The first report has demonstrated that the SGLT2 inhibitor, tofogliflozin, reduced albuminuria and glomerular hypertrophy in *db/db* mice [22]. The second report has shown that luseogliflozin slowed the progression of diabetic nephropathy in a type 2 diabetic rat model [27]. However, neither inflammation nor oxidative stress in renal tissue or in cultured renal cells was examined in these studies. To the best of our knowledge, this is the first study to investigate the protective effects of an SGLT2 inhibitor on diabetic nephropathy by inhibiting inflammation and oxidative stress by both *in vivo* and *in vitro* experiments.

Vallon *et al.* have shown that SGLT2 knockout attenuated hyperglycemia and glomerular hyperfiltration, but not renal injury, oxidative stress and inflammation in the streptozotocin (STZ)-induced type 1 diabetes model [28]. There are two possibilities for the discrepancy between their results and ours. First, it is well known that STZ has toxicity and that STZ itself may affect the kidney and induce renal injury, oxidative stress and inflammation. Second, the glucose level was lower in the STZ-induced diabetic SGLT2-knockout mice than in the diabetic wild-type mice (300 vs. 470 mg/dl); however, it was still much higher than the normal level. The glucose level in their diabetic SGLT2-knockout mice was similar to that in our untreated *db/db* mice. Therefore, hyperglycemia per se may induce oxidative stress, inflammation and renal injury. A recent clinical study has reported that empagliflozin ameliorated hyperfiltration, but not the urine albumin/creatinine ratio in patients with type 1 diabetes [29]. The treatment period in this study was only 8 weeks, which is too short to expect the effect of an SGLT2 inhibitor to reduce albuminuria. Furthermore, we should be careful not to administer SGLT2 inhibitors to type 1 diabetic patients, as SGLT2 inhibitors are indicated in patients with type 2 diabetes mellitus at present.

Tahara *et al.* have reported that the SGLT2 inhibitor, ipragliflozin, reduced plasma and liver levels of oxidative stress biomarkers and inflammatory markers, and ameliorated hyperglycemia in a mouse model of diabetes [30]. Chen *et al.* have shown that the SGLT2 inhibitor, BI-38335, suppressed the gene expression of inflammatory cytokines in pancreas, and improved glycemic control in *db/db* mice [15]. However, the effects of SGLT2 inhibitors on oxidative stress and inflammation in diabetic nephropathy were not investigated in these studies. To elucidate the precise mechanisms by which dapagliflozin inhibits diabetes-induced inflammation and oxidative stress, and thus ameliorates diabetic nephropathy, further investigations are needed.

In conclusion, we demonstrated that the SGLT2 inhibitor, dapagliflozin, ameliorates the characteristic changes of diabetic nephropathy and reduces albuminuria, as well as hyperglycemia and β-cell damage in *db/db* mice. Dapagliflozin shows renoprotective effects through its glucose lowering effect and at least in part by anti-inflammatory/oxidative stress effects in the diabetic kidney. Our results indicate that dapagliflozin may be a therapeutic option for the management of diabetic nephropathy.

Acknowledgments

The authors thank Ms. Miwa Sato for technical assistance.

Author Contributions

Conceived and designed the experiments: DO. Performed the experiments: NT DO HT TH CSH. Analyzed the data: JW AN JE NN HY. Wrote the paper: DO KT HM.

References

1. Gilbertson DT, Liu J, Xue JL, Louis TA, Solid CA, et al. (2005) Projecting the number of patients with end-stage renal disease in the United States to the year 2015. J Am Soc Nephrol 16: 3736–3741.
2. Kanwar YS, Sun L, Xie P, Liu FY, Chen S (2011) A glimpse of various pathogenetic mechanisms of diabetic nephropathy. Annu Rev Pathol 6: 395–423.
3. Navarro-Gonzalez JF, Mora-Fernandez C, Muros de Fuentes M, Garcia-Perez J (2011) Inflammatory molecules and pathways in the pathogenesis of diabetic nephropathy. Nat Rev Nephrol 7: 327–340.
4. Giacco F, Brownlee M (2010) Oxidative stress and diabetic complications. Circ Res 107: 1058–1070.
5. Hediger MA, Rhoads DB (1994) Molecular physiology of sodium-glucose cotransporters. Physiol Rev 74: 993–1026.
6. Wright EM (2001) Renal Na(+)-glucose cotransporters. Am J Physiol Renal Physiol 280: F10–18.
7. Chao EC, Henry RR (2010) SGLT2 inhibition–a novel strategy for diabetes treatment. Nat Rev Drug Discov 9: 551–559.
8. Chen LH, Leung PS (2013) Inhibition of the sodium glucose co-transporter-2: its beneficial action and potential combination therapy for type 2 diabetes mellitus. Diabetes Obes Metab 15: 392–402.
9. Han S, Hagan DL, Taylor JR, Xin L, Meng W, et al. (2008) Dapagliflozin, a selective SGLT2 inhibitor, improves glucose homeostasis in normal and diabetic rats. Diabetes 57: 1723–1729.
10. Bouchie A (2013) SGLT2 inhibitors enter crowded diabetes space. Nat Biotechnol 31: 469–470.
11. Plosker GL (2012) Dapagliflozin: a review of its use in type 2 diabetes mellitus. Drugs 72: 2289–2312.
12. Defronzo RA, Hompesch M, Kasichayanula S, Liu X, Hong Y, et al. (2013) Characterization of Renal Glucose Reabsorption in Response to Dapagliflozin in Healthy Subjects and Subjects With Type 2 Diabetes. Diabetes Care.
13. Fujimori Y, Katsuno K, Nakashima I, Ishikawa-Takemura Y, Fujikura H, et al. (2008) Remogliflozin etabonate, in a novel category of selective low-affinity sodium glucose cotransporter (SGLT2) inhibitors, exhibits antidiabetic efficacy in rodent models. J Pharmacol Exp Ther 327: 268–276.
14. Macdonald FR, Peel JE, Jones HB, Mayers RM, Westgate L, et al. (2010) The novel sodium glucose transporter 2 inhibitor dapagliflozin sustains pancreatic function and preserves islet morphology in obese, diabetic rats. Diabetes Obes Metab 12: 1004–1012.
15. Chen L, Klein T, Leung PS (2012) Effects of combining linagliptin treatment with BI-38335, a novel SGLT2 inhibitor, on pancreatic islet function and inflammation in db/db mice. Curr Mol Med 12: 995–1004.
16. Matsushita Y, Ogawa D, Wada J, Yamamoto N, Shikata K, et al. (2011) Activation of peroxisome proliferator-activated receptor delta inhibits streptozotocin-induced diabetic nephropathy through anti-inflammatory mechanisms in mice. Diabetes 60: 960–968.
17. Okada S, Shikata K, Matsuda M, Ogawa D, Usui H, et al. (2003) Intercellular adhesion molecule-1-deficient mice are resistant against renal injury after induction of diabetes. Diabetes 52: 2586–2593.
18. Ogawa D, Asanuma M, Miyazaki I, Tachibana H, Wada J, et al. (2011) High glucose increases metallothionein expression in renal proximal tubular epithelial cells. Exp Diabetes Res 2011: 534872.
19. Kodera R, Shikata K, Kataoka HU, Takatsuka T, Miyamoto S, et al. (2011) Glucagon-like peptide-1 receptor agonist ameliorates renal injury through its anti-inflammatory action without lowering blood glucose level in a rat model of type 1 diabetes. Diabetologia 54: 965–978.
20. Whaley JM, Tirmenstein M, Reilly TP, Poucher SM, Saye J, et al. (2012) Targeting the kidney and glucose excretion with dapagliflozin: preclinical and clinical evidence for SGLT2 inhibition as a new option for treatment of type 2 diabetes mellitus. Diabetes Metab Syndr Obes 5: 135–148.
21. Jurczak MJ, Lee HY, Birkenfeld AL, Jornayvaz FR, Frederick DW, et al. (2011) SGLT2 deletion improves glucose homeostasis and preserves pancreatic beta-cell function. Diabetes 60: 890–898.
22. Nagata T, Fukuzawa T, Takeda M, Fukazawa M, Mori T, et al. (2013) Tofogliflozin, a novel sodium-glucose co-transporter 2 inhibitor, improves renal and pancreatic function in db/db mice. Br J Pharmacol 170: 519–531.
23. Vlassara H, Cai W, Chen X, Serrano EJ, Shobha MS, et al. (2012) Managing chronic inflammation in the aging diabetic patient with CKD by diet or sevelamer carbonate: a modern paradigm shift. J Gerontol A Biol Sci Med Sci 67: 1410–1416.
24. Ohga S, Shikata K, Yozai K, Okada S, Ogawa D, et al. (2007) Thiazolidinedione ameliorates renal injury in experimental diabetic rats through anti-inflammatory effects mediated by inhibition of NF-kappaB activation. Am J Physiol Renal Physiol 292: F1141–1150.
25. Tachibana H, Ogawa D, Matsushita Y, Bruemmer D, Wada J, et al. (2012) Activation of liver X receptor inhibits osteopontin and ameliorates diabetic nephropathy. J Am Soc Nephrol 23: 1835–1846.
26. Forbes JM, Cooper ME (2013) Mechanisms of diabetic complications. Physiol Rev 93: 137–188.
27. Kojima N, Williams JM, Takahashi T, Miyata N, Roman RJ (2013) Effects of a new SGLT2 inhibitor, luseogliflozin, on diabetic nephropathy in T2DN rats. J Pharmacol Exp Ther 345: 464–472.
28. Vallon V, Rose M, Gerasimova M, Satriano J, Platt KA, et al. (2013) Knockout of Na-glucose transporter SGLT2 attenuates hyperglycemia and glomerular hyperfiltration but not kidney growth or injury in diabetes mellitus. Am J Physiol Renal Physiol 304: F156–167.
29. Cherney DZ, Perkins BA, Soleymanlou N, Maione M, Lai V, et al. (2014) Renal hemodynamic effect of sodium-glucose cotransporter 2 inhibition in patients with type 1 diabetes mellitus. Circulation 129: 587–597.
30. Tahara A, Kurosaki E, Yokono M, Yamajuku D, Kihara R, et al. (2013) Effects of SGLT2 selective inhibitor ipragliflozin on hyperglycemia, hyperlipidemia, hepatic steatosis, oxidative stress, inflammation, and obesity in type 2 diabetic mice. Eur J Pharmacol 715: 246–255.

Am J Physiol Renal Physiol 306: F105–F115, 2014.
First published October 23, 2013; doi:10.1152/ajprenal.00034.2013.

Metallothionein deficiency exacerbates diabetic nephropathy in streptozotocin-induced diabetic mice

Hiromi Tachibana,[1] Daisuke Ogawa,[1,2] Norio Sogawa,[3] Masato Asanuma,[4] Ikuko Miyazaki,[4] Naoto Terami,[1] Takashi Hatanaka,[1] Chikage Sato Horiguchi,[1] Atsuko Nakatsuka,[1,2] Jun Eguchi,[1] Jun Wada,[1] Hiroshi Yamada,[5] Kohji Takei,[5] and Hirofumi Makino[1]

[1]*Department of Medicine and Clinical Science, Okayama University Graduate School of Medicine, Dentistry, and Pharmaceutical Sciences, Okayama, Japan;* [2]*Department of Diabetic Nephropathy, Okayama University Graduate School of Medicine, Dentistry, and Pharmaceutical Sciences, Okayama, Japan;* [3]*Department of Dental Pharmacology, Okayama University Graduate School of Medicine, Dentistry, and Pharmaceutical Sciences, Okayama, Japan;* [4]*Department of Brain Science, Okayama University Graduate School of Medicine, Dentistry, and Pharmaceutical Sciences, Okayama, Japan; and* [5]*Department of Neuroscience, Okayama University Graduate School of Medicine, Dentistry, and Pharmaceutical Sciences, Okayama, Japan*

Submitted 17 January 2013; accepted in final form 17 October 2013

Tachibana H, Ogawa D, Sogawa N, Asanuma M, Miyazaki I, Terami N, Hatanaka T, Horiguchi CS, Nakatsuka A, Eguchi J, Wada J, Yamada H, Takei K, Makino H. Metallothionein deficiency exacerbates diabetic nephropathy in streptozotocin-induced diabetic mice. *Am J Physiol Renal Physiol* 306: F105–F115, 2014. First published October 23, 2013; doi:10.1152/ajprenal.00034.2013.—Oxidative stress and inflammation play important roles in diabetic complications, including diabetic nephropathy. Metallothionein (MT) is induced in proximal tubular epithelial cells as an antioxidant in the diabetic kidney; however, the role of MT in renal function remains unclear. We therefore investigated whether MT deficiency accelerates diabetic nephropathy through oxidative stress and inflammation. Diabetes was induced by streptozotocin injection in MT-deficient ($MT^{-/-}$) and $MT^{+/+}$ mice. Urinary albumin excretion, histological changes, markers for reactive oxygen species (ROS), and kidney inflammation were measured. Murine proximal tubular epithelial (mProx24) cells were used to further elucidate the role of MT under high-glucose conditions. Parameters of diabetic nephropathy and markers of ROS and inflammation were accelerated in diabetic $MT^{-/-}$ mice compared with diabetic $MT^{+/+}$ mice, despite equivalent levels of hyperglycemia. MT deficiency accelerated interstitial fibrosis and macrophage infiltration into the interstitium in the diabetic kidney. Electron microscopy revealed abnormal mitochondrial morphology in proximal tubular epithelial cells in diabetic $MT^{-/-}$ mice. In vitro studies demonstrated that knockdown of MT by small interfering RNA enhanced mitochondrial ROS generation and inflammation-related gene expression in mProx24 cells cultured under high-glucose conditions. The results of this study suggest that MT may play a key role in protecting the kidney against high glucose-induced ROS and subsequent inflammation in diabetic nephropathy.

diabetic nephropathy; inflammation; metallothionein; oxidative stress; reactive oxygen species

DIABETIC NEPHROPATHY IS THE leading cause of end-stage renal disease worldwide and an independent risk factor for cardiovascular disease (10, 25). Several mechanisms contribute to the onset and progression of diabetic nephropathy, including genetic and hemodynamic factors, oxidative stress, and inflammation (4). Numerous studies have suggested that hyperglycemia is associated with enhanced generation of reactive oxygen species (ROS), and oxidative stress has been implicated in the development of diabetic nephropathy (6, 7). Emerging evidence also suggests that inflammatory pathways are crucially involved in the pathogenesis of diabetic nephropathy (20, 26). The regulation of oxidative stress and inflammation could thus represent a major therapeutic target in diabetic nephropathy.

Metallothionein (MT) is an intracellular metal-binding protein characterized by a low molecular mass (6–7 kDa), high cysteine content (20 of 61–62 amino acids), and no aromatic or histidine residues (30). Although four isoforms have been characterized, MT-1 and -2 (MT-1/-2) are widely distributed as the major isoforms throughout the body (30). MT plays an important role in heavy metal detoxification and essential metal homeostasis (24). In addition, MT has a potent antioxidant function and is an adaptive protein that protects cells and tissues from oxidative stress (2, 9). Previous studies have reported neuroprotective effects of MT in mouse models of Parkinson's disease (5, 17, 18). We recently demonstrated that MT was expressed mainly in renal proximal tubular epithelial cells and that high-glucose-induced oxidative stress may enhance the expression of MT in the diabetic kidney (21). These results suggest that MT is upregulated in compensation to protect kidneys from oxidative stress induced by diabetic conditions; however, the role of MT in the pathogenesis of diabetic nephropathy remains poorly understood.

The present study therefore aimed to investigate the role of MT in protecting the kidney from high-glucose-induced oxidative stress under diabetic conditions, using MT deficient ($MT^{-/-}$) and $MT^{+/+}$ mice. We also used murine proximal tubular epithelial (mProx24) cells cultured under normal- or high-glucose conditions to determine whether knockdown of MT by small interfering RNA (siRNA) induced mitochondrial ROS, leading to inflammation.

MATERIALS AND METHODS

Experimental protocol. Male homozygous MT-1/-2 knockout ($MT^{-/-}$) mice were obtained from Jackson Laboratory (Bar Harbor, ME). The $MT^{-/-}$ mice were raised on a 129/Sv genetic background, and 129/Sv mice were therefore used as wild-type controls ($MT^{+/+}$). All procedures were performed according to the Guidelines for Animal Experiments at Okayama University Medical School, the Japa-

Address for reprint requests and other correspondence: D. Ogawa, Depts. of Medicine and Clinical Science and Diabetic Nephropathy, Okayama Univ. Graduate School of Medicine, Dentistry, and Pharmaceutical Sciences, 2-5-1 Shikata-cho, Kita-ku, Okayama 700-8558, Japan (e-mail: daiogawa@md.okayama-u.ac.jp).

Table 1. *Metabolic data at 12 wk after induction of diabetes*

	Nondiabetic		Diabetic	
	$MT^{+/+}$	$MT^{-/-}$	$MT^{+/+}$	$MT^{-/-}$
Urinary albumin excretion, μg/day	23.45 ± 2.43	19.01 ± 2.50	92.92 ± 14.76*	120.66 ± 18.66†‡
Body weight, g	30.45 ± 0.27	30.15 ± 0.57	22.93 ± 2.03*	23.68 ± 1.09†
Kidney weight, mg	430 ± 1.6	426 ± 1.4	493 ± 3.3	475 ± 2.4
Relative kidney weight, mg/g body weight	14.11 ± 0.41	14.12 ± 0.34	21.67 ± 1.04*	20.22 ± 0.87†
Glycated hemoglobin, %	3.60 ± 0.04	3.37 ± 0.06	6.20 ± 0.46*	6.05 ± 0.18†

Values are means ± SE; MT, metallothionein. *$P < 0.01$ vs. nondiabetic $MT^{+/+}$. †$P < 0.01$ vs. nondiabetic $MT^{-/-}$. ‡$P < 0.05$ vs. diabetic $MT^{+/+}$.

nese Government Animal Protection and Management Law (No. 105), and Japanese Government Notification on Feeding and Safekeeping of Animals (No. 6). Eight-week-old mice were divided into four groups: *1*) nondiabetic $MT^{+/+}$ mice (ND-WT; $n = 7$); *2*) streptozotocin (STZ)-induced diabetic $MT^{+/+}$ mice (DM-WT; $n = 7$); *3*) nondiabetic $MT^{-/-}$ mice (ND-KO; $n = 7$); and *4*) diabetic $MT^{-/-}$ mice (DM-KO; $n = 7$). Diabetes was induced and confirmed as reported previously (15). All mice had free access to a standard diet and tap water. Mice were euthanized at 12 wk after the induction of diabetes. The kidneys were removed, weighed, and fixed in 10% formalin for periodic acid-methenamine silver (PAM) and Masson trichrome staining. Parts of the remaining tissues were embedded in optimal cutting temperature compound (Sakura Finetechnical, Tokyo, Japan) and frozen immediately in acetone, cooled on dry ice. Other tissues were snap-frozen in liquid nitrogen and stored at −80°C.

To explore the effect of STZ on diabetic nephropathy, 8-wk-old $MT^{-/-}$ mice were divided into three groups: *1*) nondiabetic mice (ND-KO; $n = 5$); *2*) STZ-induced diabetic mice (DM-KO; $n = 5$); and *3*) STZ-induced diabetic mice treated with insulin glargine (DM-KO+glargine; $n = 5$). Insulin glargine (Sanofi, Tokyo, Japan) was administered 0.5–0.8 U/body intraperitoneally. Mice were euthanized at 12 wk after the induction of diabetes. The kidneys were removed and fixed in 10% formalin for PAM staining.

Metabolic data. Body weight, kidney weight, glycated hemoglobin, serum creatinine, and 24-h urinary albumin excretion (UAE) were measured at 12 wk. Glycated hemoglobin was measured using high-pressure liquid chromatography, and serum creatinine was measured using an enzymatic method. Urine was collected for 24 h, with each mouse housed individually in a metabolic cage and provided with food and water ad libitum. UAE was measured as previously described (22).

Light microscopy. Sections were analyzed by PAM and Masson trichrome staining. Glomerular size was estimated by examining 10 randomly selected glomeruli in the cortex per animal under high magnification (×400) at 12 wk after induction of diabetes. The area of the glomerular tuft and interstitial fibrosis was measured using Lumina Vision software (Mitani, Tokyo, Japan). The mesangial matrix index (MMI) was defined as the PAM-positive area in the tuft area, calculated using the following formula: MMI = (PAM-positive area)/(tuft area). The results are expressed as means ± SE (per μm^2 for tuft area; arbitrary units for MMI).

Immunoperoxidase staining. Immunoperoxidase staining was performed as described previously (22). Briefly, fresh frozen sections were cut at 4-μm thickness using a cryostat. Macrophage infiltration was evaluated using a rat anti-mouse monocyte/macrophage (F4/80) monoclonal antibody (Abcam, Cambridge, UK), followed by a biotin-labeled goat anti-rat IgG antibody (Jackson ImmunoResearch Laboratories, West Grove, PA). The avidin-biotin coupling reaction was performed on sections using a Vectastain Elite kit (Vector Laboratories, Burlingame, CA). We counted the number of F4/80-positive cells in 10 glomeruli/animal. The mean number of positive cells per glomerulus and interstitial tissue (number per mm^2) were used for the estimation.

Immunofluorescent staining. Immunofluorescent staining was performed as described previously (21). Renal expression of MT-1/-2 was detected using a rabbit anti-MT antibody (Santa Cruz Biotechnology, Santa Cruz, CA) followed by Alexa Fluor 488 donkey anti-rabbit IgG (Invitrogen, Carlsbad, CA). To determine whether MT-1/-2 was localized in proximal or distal tubular epithelial cells, the sections were counterstained with goat anti-aquaporin-1 (AQP1) antibody (Santa Cruz Biotechnology) or goat anti-Tamm-Horsfall protein (THP) antibody (Santa Cruz Biotechnology), respectively, followed by Alexa Fluor 594 donkey anti-goat IgG (Invitrogen). For other immunofluorescent staining, anti-type IV collagen (Millipore, Temecula, CA), anti-fibronectin (Sigma-Aldrich, St. Louis, MO), and anti-4-hydroxynonenal (4-HNE; Abcam) were used. Fluorescence images were obtained using a fluorescence microscope (BX51; Olympus, Tokyo, Japan).

Western blot analysis. Western blotting was performed as previously described (15). Briefly, the proteins were eluted, resolved by SDS-PAGE, and transferred to nitrocellulose membranes. After blocking in 20 mM Tris·HCl (pH 7.6) containing 150 mM NaCl, 0.1% Tween 20, and 5% (wt/vol) nonfat drt milk, the membranes were incubated with anti-fibronectin (Sigma-Aldrich) and anti-phospho-NF-κB-p65 (Cell Signaling Technology, Danvers, MA). The membranes were hybridized with anti-β-actin (Abcam) to monitor equivalent loading in different lanes. All experiments were repeated at least three times.

Electron microscopy. Tissue preparation for electron microscopy was performed as described previously (22). The proximal tubular epithelial cells were photographed at magnifications of ×1,500 and ×4,000.

Fig. 1. Interstitial fibrosis was accelerated in diabetic metallothionein (MT)-deficient mice. *A*: representative photomicrographs of periodic acid-methenamine silver (PAM), type IV collagen, Masson's trichrome, and fibronectin staining. ND-WT, nondiabetic $MT^{+/+}$ mice; ND-KO, nondiabetic $MT^{-/-}$ mice; DM-WT, diabetic $MT^{+/+}$ mice; DM-KO, diabetic $MT^{-/-}$ mice. Original magnifications: ×400 for PAM and type IV collagen staining and ×100 for Masson's trichrome and fibronectin staining. *B* and *C*: quantitative analysis of the mesangial matrix index (MMI) and type IV collagen-positive area in the glomeruli. Glomerular hypertrophy and mesangial matrix expansion were evident in DM-WT and DM-KO. Values are means ± SE. **$P < 0.01$. *D* and *E*: quantitative analysis of interstitial fibrosis- and fibronectin-positive area in the interstitium. Interstitial fibrosis was evident in diabetic mice and was significantly increased in DM-KO compared with DM-WT. Values are means ± SE. *$P < 0.05$, **$P < 0.01$. *F*: Western blot analysis of fibronectin protein expression. Fibronectin is significantly upregulated in DM-KO compared with ND-KO. Quantification was performed by densitometry of 3 independently performed experiments with normalization by β-actin. Values are means ± SE. *$P < 0.05$. *G*: representative photomicrographs of Masson's trichrome staining. ND-KO, nondiabetic $MT^{-/-}$ mice; DM-KO, diabetic $MT^{-/-}$ mice; DM-KO+glargine, diabetic mice treated with insulin glargine. Original magnification, ×100. *H*: quantitative analysis of interstitial fibrosis. Interstitial fibrosis was evident in DM-KO and was significantly decreased in DM-KO+glargine compared with DM-KO. Values are means ± SE. **$P < 0.01$.

Quantitative analysis of renal cortex gene expression. RNA was isolated from the renal cortex 12 wk after treatment using an RNeasy Mini kit (Qiagen, Valencia, CA). Single-strand cDNA was synthesized from the extracted RNA using an RT-PCR kit (PerkinElmer, Foster City, CA). Quantitative RT-PCR (qRT-PCR) was performed to analyze the mRNA expression of CD14, monocyte chemoattractant protein (MCP)-1, transforming growth factor (TGF)-β, and osteopontin (OPN) in the renal cortex, using StepOnePlus (Applied Biosys-

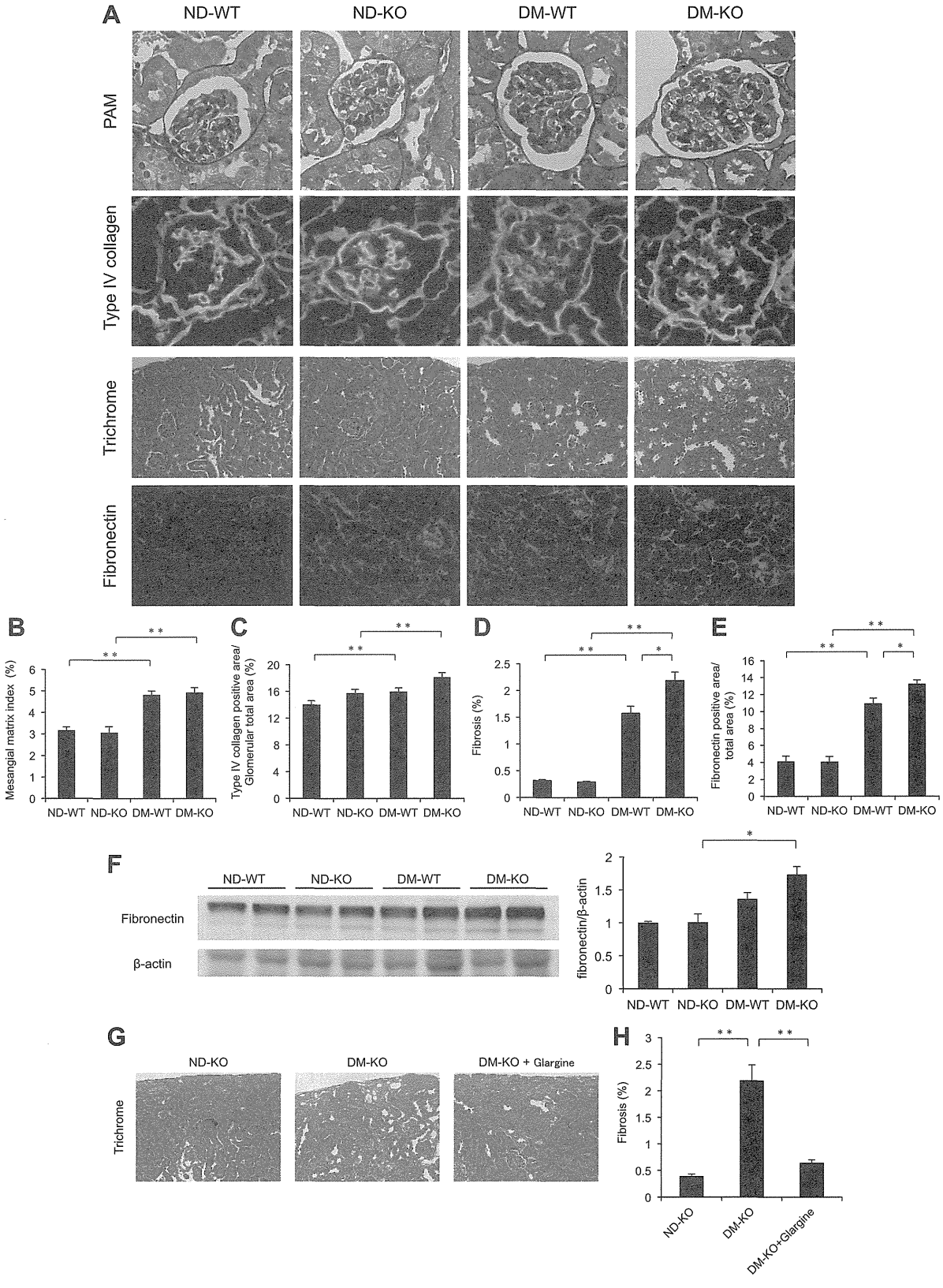

tems, Tokyo, Japan) and FastStart SYBR Premix Ex Taq II (Takara Bio, Otsu, Japan). The primers were purchased from Takara Bio. The results of qRT-PCR were evaluated by the comparative Ct method using GAPDH as the invariant control gene.

Mitochondrial ROS detection. Mitochondrial ROS were detected using MitoTracker Red CM-H_2XRos (Molecular Probes, Eugene, OR) and MitoTracker Green FM (Molecular Probes). Briefly, renal sections were incubated with 10 μM MitoTracker Red CM-H_2XRos and MitoTracker Green FM at room temperature for 1 h. Unbound dye was then removed, and fluorescence was analyzed using a fluorescence microscope (BX51; Olympus, Tokyo, Japan).

Cell culture and treatment. Murine proximal tubular epithelial (mProx24) cells were generously provided by Dr. Takeshi Sugaya (CMIC) and cultured as reported previously (21). mProx24 cells were cultured in DMEM supplemented with 5.5 mM D-glucose (low glucose), 10% FBS, 100 U/ml penicillin, 100 mg/ml streptomycin, and 2 mM L-glutamine. siRNA experiments were performed using MT siRNA (sc-35926; Santa Cruz Biotechnology) and scrambled siRNA (sc-37007; Santa Cruz Biotechnology). mProx24 cells were transfected with 12.5 nM MT siRNA or scrambled siRNA in the presence of Lipofectamine RNAiMAX (Invitrogen). After siRNA transfection for 24 h, the cells were stimulated with 25 mM D-glucose (high glucose) for 24 h. Individual experiments were repeated at least three times with different lots or preparation of cells.

Quantitative analysis of gene expression in mProx24 cells. Total RNA was prepared from cells using an RNeasy Mini kit (Qiagen) as described above. Nox4, MCP-1, TGF-β, and OPN mRNA expression levels in mProx24 cells were measured using qRT-PCR, as described above.

ELISA. Levels of MT-1/-2 in kidney tissue and mProx24 cells were measured by an ELISA system (Frontier Science, Ishikari, Japan) according to the manufacturer's protocol.

Statistical analysis. All values are given as means ± SE. Statistically significant differences between groups were examined using one-way ANOVA followed by Scheffé's test. A P value <0.05 was considered statistically significant.

RESULTS

STZ induced greater renal damage in $MT^{-/-}$ mice compared with $MT^{+/+}$ mice. The metabolic data are summarized in Table 1. The UAE was significantly higher in diabetic mice than in nondiabetic mice. Moreover, UAE was significantly increased in diabetic $MT^{-/-}$ mice compared with diabetic $MT^{+/+}$ mice at 12 wk after STZ injection (120.66 ± 18.66 vs. 92.92 ± 14.76 μg/day; $p < 0.05$). Glycated hemoglobin and relative kidney weight were increased and body weight was decreased in diabetic mice compared with nondiabetic mice. There were no significant differences in glycated hemoglobin, relative kidney weight, and body weight between diabetic $MT^{+/+}$ mice and diabetic $MT^{-/-}$ mice.

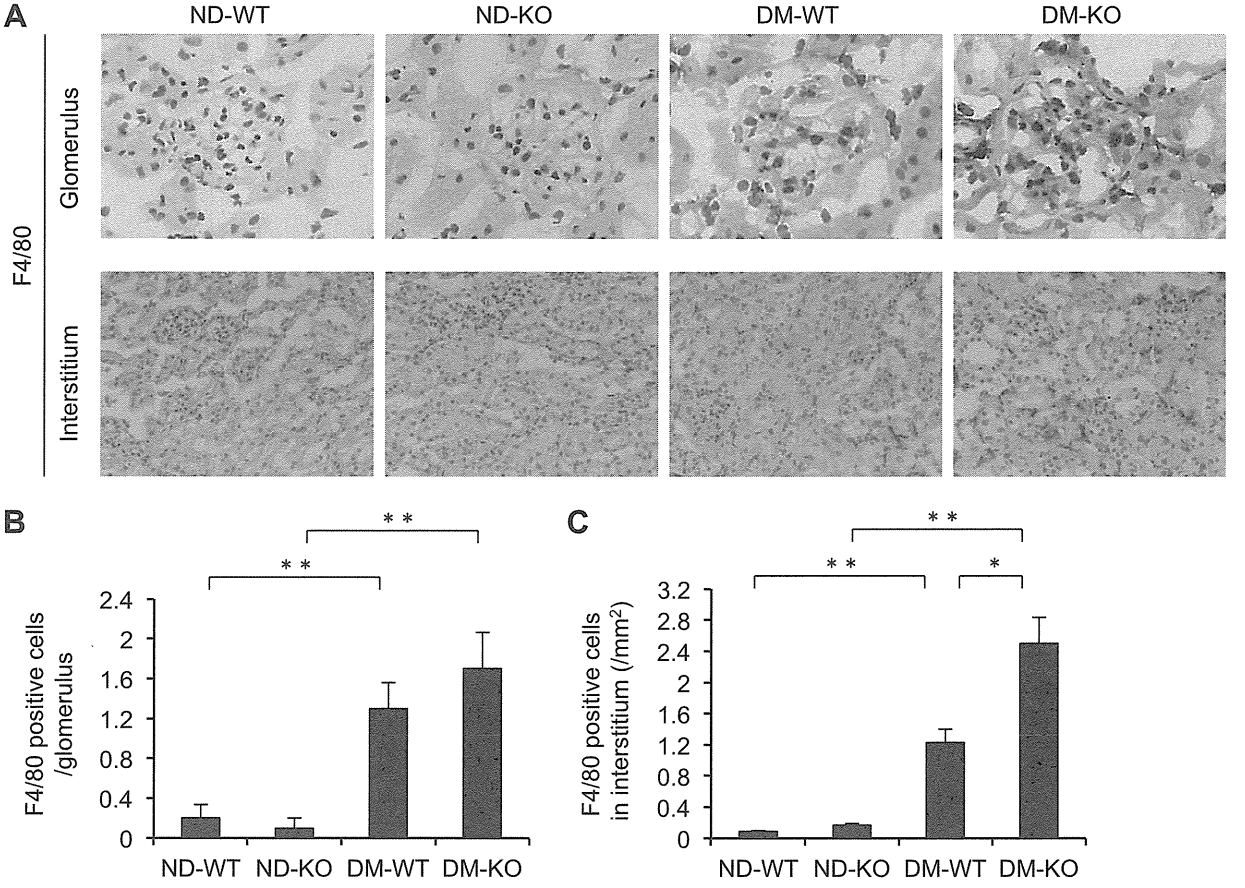

Fig. 2. MT deficiency promotes macrophage infiltration into the interstitium in diabetic mice. *A*: macrophage infiltration into the glomeruli and the interstitium was clearly evident in diabetic mice and was significantly increased in DM-KO compared with DM-WT in the interstitium. Original magnifications: ×400 for glomeruli and ×100 for interstitium. *B*: number of intraglomerular macrophages. Values are means ± SE. $^{**}P < 0.01$. *C*: number of macrophages in the interstitium. Values are means ± SE. $^{*}P < 0.05$. $^{**}P < 0.01$.

STZ induced more severe interstitial fibrosis in $MT^{-/-}$ mice compared with $MT^{+/+}$ mice. Kidneys were isolated and processed for pathological analysis using PAM staining, Masson's trichrome staining, and immunofluorescence for type IV collagen and fibronectin (Fig. 1*A*). As revealed by PAM and type IV collagen staining, glomerular hypertrophy and mesangial matrix expansion were clearly observed in both $MT^{+/+}$ and $MT^{-/-}$ mice after STZ injection. However, morphometric analysis of PAM and the type IV collagen-positive area showed no significant differences between $MT^{-/-}$ and $MT^{+/+}$ mice (Fig. 1, *B* and *C*). Masson's trichrome staining showed significantly increased interstitial fibrosis in diabetic $MT^{+/+}$ mice, which was further increased in diabetic $MT^{-/-}$ mice (1.58 ± 0.13 vs. $2.18 \pm 0.16\%$; $P < 0.05$) (Fig. 1*D*). Immunofluorescent staining and Western blotting for fibronectin also showed the same tendency (Fig. 1, *E* and *F*). Furthermore, interstitial fibrosis in diabetic $MT^{-/-}$ mice was attenuated by insulin treatment, suggesting that interstitial fibrosis observed in STZ-induced diabetic mice was mediated by hyperglycemia (Fig. 1, *G* and *H*). Collectively, these results demonstrate that MT deficiency accelerates interstitial fibrosis in STZ-induced diabetes.

Macrophage infiltration into the interstitium was increased in diabetic $MT^{-/-}$ mice compared with diabetic $MT^{+/+}$ mice. The numbers of macrophages in both the glomeruli and interstitium were remarkably higher in diabetic mice compared with nondiabetic mice (Fig. 2*A*). There was no difference in macrophage infiltration into the glomeruli in response to STZ treatment between $MT^{-/-}$ and $MT^{+/+}$ mice (Fig. 2*B*). However, macrophage infiltration into the interstitium was increased in diabetic $MT^{-/-}$ mice compared with diabetic $MT^{+/+}$ mice (2.50 ± 0.34 vs. 1.23 ± 0.18; $P < 0.01$) (Fig. 2*C*). These findings indicate that MT deficiency accelerates macrophage infiltration into the interstitium of the diabetic kidney.

MT-1/-2 expression was increased in diabetic $MT^{+/+}$ mice. We determined the levels of MT-1/-2 in kidney tissue by ELISA (Fig. 3*A*). The MT-1/-2 level in renal tissue was strongly upregulated in diabetic $MT^{+/+}$ mice compared with control $MT^{+/+}$ mice. In contrast, MT-1/-2 was hardly detected in the kidneys of control and diabetic $MT^{-/-}$ mice. To localize MT-1/-2 in the diabetic $MT^{+/+}$ kidney, we performed double immunofluorescence for MT-1/-2, and AQP1 (a marker of proximal tubular epithelial cells) or THP (a marker of distal tubular epithelial cells). As shown in Fig. 3*B*, MT-1/-2 was predominantly localized in the proximal tubular epithelial cells, and to a lesser extent in the distal tubular epithelial cells of the diabetic kidney.

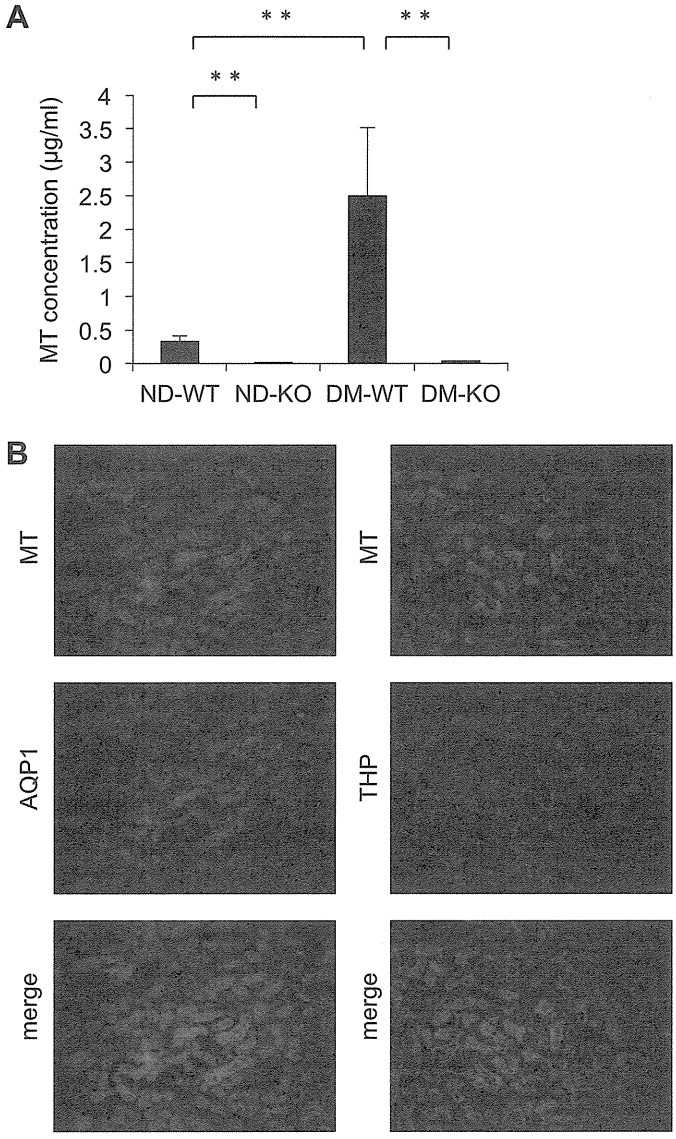

Fig. 3. MT-1/-2 expression is upregulated in the diabetic kidney. *A*: ELISA was performed as described in MATERIALS AND METHODS. Twelve weeks after induction of diabetes, MT-1/-2 was predominantly expressed in the renal cortex of DM-WT compared with ND-WT. In contrast, MT-1/-2 was hardly detected in the kidneys of ND-KO and DM-KO. Values are means ± SE. $^{**}P < 0.01$. *B*: representative photomicrographs of double immunofluorescent staining. MT-1/-2 expression was predominantly localized in the proximal tubular epithelial cells, and to a lesser extent in the distal tubular epithelial cells of the diabetic kidneys. Original magnifications: ×100.

Macrophage and inflammatory gene expression in the renal cortex were higher in diabetic $MT^{-/-}$ mice compared with diabetic $MT^{+/+}$ mice. qRT-PCR analyses of kidney tissues demonstrated increased gene expression of the macrophage marker CD14 in the diabetic groups, and expression of this gene was increased in diabetic $MT^{-/-}$ mice compared with diabetic $MT^{+/+}$ mice (Fig. 4*A*). Similarly, diabetes induction increased the renal expression of several proinflammatory and proatherogenic genes, including MCP-1, TGF-β, and OPN (Fig. 4, *B–D*). Notably, MCP-1 is a key chemokine involved in macrophage recruitment that plays a significant role in diabetic nephropathy, and the absence of MCP-1 significantly reduces diabetic renal injury. Similarly, TGF-β and OPN are also critical inflammatory cytokines involved in diabetic nephropathy. To investigate the involvement of NF-κB in the induction of inflammatory cytokines, we performed Western blotting. The expression of NF-κB was increased in diabetic $MT^{-/-}$ mice compared with diabetic $MT^{+/+}$ mice (Fig. 4*E*). Collectively, these data indicate that MT deficiency accelerates diabetes-induced macrophage recruitment and inflammatory gene expression in the kidney.

Renal ROS generation was increased in diabetic $MT^{-/-}$ mice compared with diabetic $MT^{+/+}$ mice. To evaluate oxidative stress in the kidney, renal sections were immunostained for 4-HNE. This revealed that ROS were generated predominantly in tubular epithelial cells of diabetic $MT^{+/+}$ and $MT^{-/-}$ mice,